1-Dimensional behavior and sliding Luttinger liquid phase in a frustrated spin-1/2 crossed chain model: contribution of exact diagonalizations.

P. Sindzingre, J.-B. Fouet, C. Lhuillier

Laboratoire de Physique Théorique des Liquides-UMR 7600 of CNRS, Université Pierre et Marie Curie, case 121, 4 place Jussieu, 75252 Paris Cedex, France

E-mail:phsi@lptl.jussieu.fr

Exact diagonalizations indicate that the effective 1-dimensional behavior (sliding Luttinger liquid phase) of the frustrated spin-1/2 crossed chain model, predicted by Starykh, Singh and Levine [Phys. Rev. Lett. **88**, 167203 (2002)], persists for a wide range of transverse couplings. The extension of the other phases (plaquette valence bond crystal and Néel long range order) is precised. No clear indication of a coexistence of these two phases is found, at variance with a suggestion of Sachdev and Park (cond-mat/0108214).

PACS numbers: 75.10.Jm; 75.50.Ee; 75.40.-s

I. INTRODUCTION

Among the family of frustrated two dimensional spin-1/2 antiferromagnetic (AF) models, a crossed chain model (CCM), which may also be viewed as an extension of the checkerboard antiferromagnet, has recently attracted interest in two distinct ranges of parameter [1–4]. The CCM Hamiltonian reads:

$$\mathcal{H} = J_1 \sum_{<i,j>} \mathbf{S}_i.\mathbf{S}_j + J_2 \sum_{<<i,j>>} \mathbf{S}_i.\mathbf{S}_j \qquad (1.1)$$

where the exchange J_1 couple nearest-neighbor pairs $< i, j >$ of spins on a square lattice and exchange J_2 next-nearest-neighbor pairs $<< i, j >>$ on a checkerboard pattern of plaquettes as shown in Fig. 1. Alternatively, J_2 may be viewed as the intra-chain exchange between spins on the diagonal chains and J_1 as the coupling constant between these crossed chains. Both J_1 and J_2 are assumed positive, describing AF couplings. This model interpolates between the AF Heisenberg model on the square lattice for $J_2 = 0$ and decoupled AF Heisenberg chains for $J_1 = 0$. When $J_1 = J_2$, one has the checkerboard antiferromagnet which is a 2d analog of the pyrochlore antiferromagnet.

The physics of the spin-1/2 model is well established at three points. For $J_2 = 0$ it has collinear Néel long range order (LRO) with gapless $\Delta S^z = 1$ elementary excitations (magnons). At $J_2 = J_1$ it is a valence bond crystal (VBC) with LRO in singlet plaquettes [4]; its elementary excitations are gapped and carry integer spins [5]. When $J_2/J_1 = \infty$, one has the physics of decoupled AF Heisenberg chains, their elementary excitations are gapless spin-1/2 deconfined spinons.
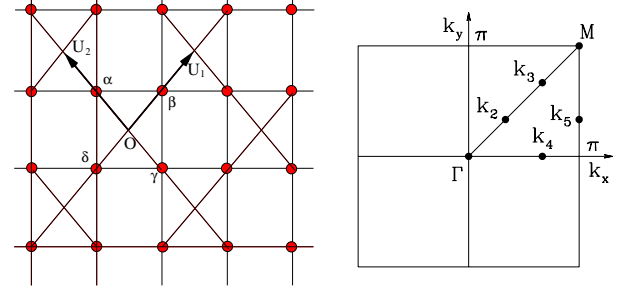

FIG. 1. Left: the crossed chain magnet. The spins sit at the vertices shown by bullets, the coupling constant between nearest-neighbor pairs is J_1, the coupling constant on the diagonal bonds of the checkerboard of plaquettes is J_2. $\mathbf{u_1}, \mathbf{u_2}$ are the unit vectors of the Bravais lattice. Right: the Brillouin zone associated to this lattice. Γ, k_i ($i = 2, 5$), M are the six different wave vectors present in the N=36 sample.

Recently, motivated by experimental results on Cs_2CuCl_4 [7] and $Na_2Ti_2Sb_2O$ [8], Starykh, Singh and Levine (SSL) have investigated the CCM in the limit $J_2/J_1 \gg 1$ where it describes "weakly" coupled chains [1]. They concluded that, the chains behave then as quasi-decoupled, realizing a $SU(2)$ "sliding Luttinger phase" [13,14]. Usually the 1d AF Heisenberg behavior is unstable to non frustrating 2d couplings giving rise to Néel LRO or VBC LRO. SSL argue that in the CCM the 1d behavior should survive for finite non negligible J_1/J_2 due to the frustrating nature of the transverse coupling. Since the pioneering works of Majumdar-Gosh and Haldane, many ladder models have been studied giving birth to various 1d behaviors [9–11]. The case of the spatially anisotropic couplings of the triangular lattice typical of Cs_2CuCl_4, appears in some aspects rather exceptional with non negligible transverse couplings and nevertheless an effective 1d behavior with a continuum of gapless excitations looking very much like Fadeev spinons [12].

The first purpose of this paper is to investigate SSL prediction using exact diagonalizations (ED) and try to figure out the possible extension of the quasi-1d regime with decreasing J_2/J_1. The second purpose will be to study the range of stability of the VBC phase around $J_2/J_1 = 1$. We shall also address a new suggestion of Sachdev and Park [6] on the possible coexistence of phases with two different order parameters between the pure VBC and Néel phases.

II. RESULTS

The ED calculations have been carried out on $N = 16, 32, 36$ samples which display all the symmetries of the infinite lattice, using periodic boundary conditions as described in [4]. Additional calculations using twisted boundary conditions were also performed on the $N = 16$ sample (specifically for $J_2/J_1 > 1$) which indicated that the lowest ground-state energies are obtained for periodic boundary conditions: it might be inferred from these results that incommensurate phases are unlikely in the absence of a magnetic field [1].

The general evolutions, as a function of J_2 ($J_1 = 1$), of the ground-state energies per spin E/N and the spin gaps Δ are displayed in Figs. 2, 3 and 4. As shown in Fig. 2 the point of "maximum frustration" where E/N has its maximum, is reached for J_2/J_1 slightly smaller than one, close to the checkerboard point. On might notice that the finite size evolutions between N=32 and N=36 are hardly visible on the scale of these figures for $J_2/J_1 < 1$ but are dramatic for $J_2/J_1 > 1$. We will show below that this last behavior is related to the quasi- 1-dimensional behavior of the model in this range of parameter.
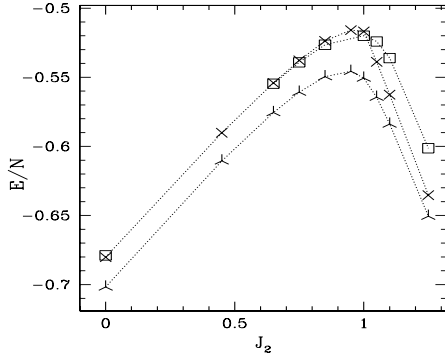

FIG. 2. Ground-state energies per spin E/N vs J_2 ($J_1 = 1$) for $J_2 \leq 1.25$: $N = 16$ (tripodes), $N = 32$ (crosses) and $N = 36$ (full squares). The dotted lines are guides for the eye.

A. Quasi 1d behavior

ED results show a large extension of 1d behavior from $J_2/J_1 = \infty$ down to $J_2/J_1 = 1.5$ and probably below.

First, Fig. 4 shows that E/N is quite close to the energy values of decoupled chains of same length for $J_2/J_1 \geq 1.10$. Comparison of results for N=16 and N=32 shows that increasing the number of chains pushes the energy per spin toward the value of uncoupled chains (Note that the N=16 sample has 2×2 chains of length 4, the N=32 sample has 2×4 chains of length 4, whereas the N=36 sample has 2×3 chains of length 6). Pointing to the same conclusion, the spin gap (Fig. 3) shows
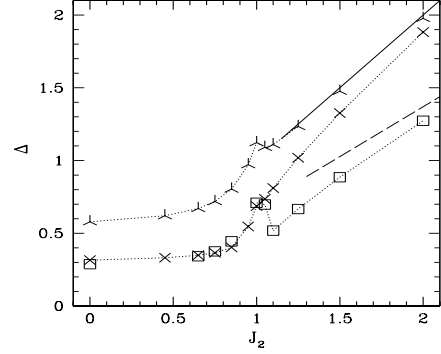

FIG. 3. Spin gap Δ vs J_2 ($J_1 = 1$), same symbols as in Fig. 2. Extra lines show the spin gap values for independent chains of length $L = 4$ (full line) and $L = 6$ (dashed line) for $J2 > 1.25$.
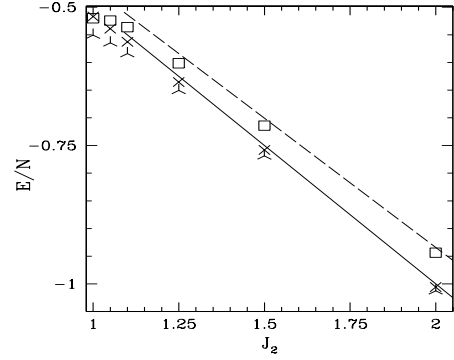

FIG. 4. Ground-state energies per spin E/N vs J_2 for $J_2 \geq 1$, same symbols as in Fig. 2. Extra lines show the E/N values for independent chains of length $L = 4$ (full line) and $L = 6$ (dashed line) for $J2 > 1.25$.

dramatic finite size effects between N=32 and N=36 for $J_2/J_1 \geq 1.10$.

Second, 1d behavior down to at least $J_2/J_1 = 1.5$ is supported by spin-spin correlations:

$$s(ij) = < \mathbf{S}_i.\mathbf{S}_j > \tag{2.1}$$

and dimer-dimer correlations patterns:

$$D(ij;kl) = < \mathbf{S}_i.\mathbf{S}_j\mathbf{S}_k.\mathbf{S}_l > - < \mathbf{S}_i.\mathbf{S}_j >< \mathbf{S}_k.\mathbf{S}_l > . \tag{2.2}$$

Values of $s(ij)$ computed in the ground-state of the $N = 36$ sample at $J_2/J_1 = 1.5$ are displayed in Table I.

They are largest and decrease slowly on a line of diagonal bonds and are quite small if sites i and j belong to different chains, even if i and j are first neighbors. Spins on parallel chains are less correlated than those on orthogonal chains which may be understood in a perturbative approach: coupling between orthogonal chains involves one "J_1" term instead of two for parallel chains.

2

j	s(ij)	j	s(ij)
36	-0.4551363204	4	-0.0228887132
15	0.1970987646	2	-0.0156898505
22	-0.2193602830	9	0.0102951567
3	0.0017845218	16	0.0029547330
10	0.0006638989	17	-0.0040816720
12	-0.0009191508		

TABLE I. Spin-spin correlations $s(ij) = < \mathbf{S}_i.\mathbf{S}_j >$ between site $i = 1$ and site j in the exact ground-state of the $N = 36$ sample for $J_2/J_1 = 1.5$. The sites are numbered as in Fig. 5. Other correlations can be deduced using C_{4v} symmetries. Correlations along a J_2 chain are displayed in the upper left corner of the table , those between orthogonal chains are in the upper right corner, those between parallel chains in the lower part.
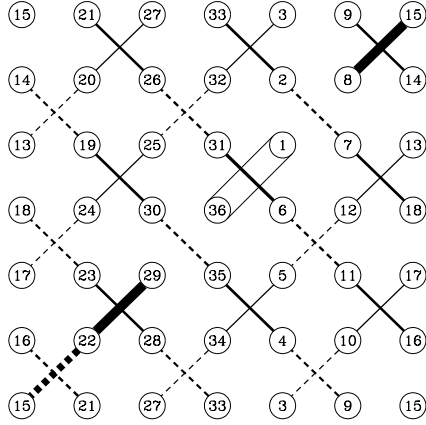

FIG. 5. Dimer-dimer correlations $D(ij; kl)$ in the exact ground-state of the $N = 36$ sample ($J_2/J_1 = 1.5$) between reference pair $(1, 36)$ and pair (k,l). Full ($D > 0$) or dashed ($D < 0$)) lines have width proportional to the square root of $|D|$ (a choice done to ease visualization).

(k,l)	D	(k,l)	D
29 22	0.0897246082	34 27	-0.0015374269
22 15	-0.0523861622	10 3	-0.0015374269
31 6	0.0110558121	34 29	-0.0011366550
35 4	0.0074567919	27 22	0.0005263317
28 23	0.0066321724	15 10	0.0005263317
16 11	0.0066321724	11 4	-0.0003686058
21 16	-0.0063063310	35 6	0.0001626070
35 30	-0.0057705738	16 9	0.0001126614
11 6	-0.0057705738	28 21	0.0001126614
9 4	-0.0046514788	35 28	-0.0000762647
17 10	0.0017481736	33 4	-0.0000456425
34 5	0.0016564513	34 3	0.0000268261
12 5	-0.0015704399	10 5	0.0000036528

TABLE II. Dimer-dimer correlations $D(ij; kl)$ (Eq. 2.2) between the pair of sites $(i, j) = (1, 36)$ and pairs of sites (k, l) in the exact ground-state of the $N = 36$ sample ($J_2 = 1.5$, $J_1 = 1$). The values of D for pairs (k, l) on diagonal bonds coupled with J_2 (left column and upper right corner above the line and Fig. 5) are all larger than on non-diagonal bonds. The sites are numbered as in Fig. 5.
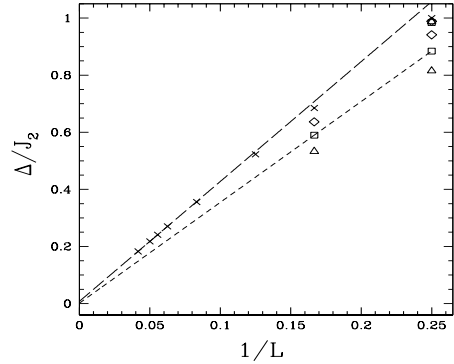

FIG. 6. Ratios Δ/J_2 of the spin-gaps to the intra-chain coupling J_2 of the chains at $J_2/J_1 = 2$ (open losanges), $J_2/J_1 = 1.5$ (open squares) and $J_2/J_1 = 1.25$ (open triangles). The spin-gaps of the AF Heisenberg chain are shown by crosses. All $N = 16$ values are very close to the $L = 4$ value of the Heisenberg chain. The dotted line joins the $N = 32$ and $N = 36$ results for $J_2/J_1 = 1.5$.

The behavior of the dimer-dimer correlations is identical (Table II and Fig. 5). $D(ij; kl)$ values between the pair (i, j) on a diagonal bond and pairs (k, l) are also largest if (i, j) and (k, l) are on the same chain. They decrease by an order of magnitude on nearby regions of crossed chains and by two orders of magnitude on parallel chains.

Third, the evolution of the spin-gap Δ with increasing size, is not inconsistent with a vanishing value for $N \to \infty$, at least down to $J_2/J_1 = 1.5$. In Fig. 6 we display the values of Δ/J_2 vs $1/L$ for $N = 16, 32$ ($L = 4$), $N = 36$ ($L = 6$) and compare them with the spin-gaps of the AF Heisenberg chain. At $J_2/J_1 = 5$ the values of Δ/J_2 (not shown) would be indistinguishable from the Heisenberg chain values and only slightly deviate from the latter down to $J_2/J_1 = 1.5$. The extrapolation for

$L \to \infty$ at $J_2/J_1 = 1.5$ is problematic due to system sizes: nevertheless a linear extrapolation of the two sets of data for $N = 32$ and $N = 36$ points to a zero gap: looking to the sign of the deviation from the $1/L$ asymptotic limit (which is negative) one is indulged to conclude that the system is still gapless in the thermodynamic limit for $J_2/J_1 = 1.5$. This could even hold at $J_2/J_1 = 1.25$, but the extrapolation is then more uncertain with present sizes.

Fourth, a lengthy but straightforward calculation shows that the quantum numbers of the ground-state and

3

first excitations of the CCM model for $J_2/J_1 = 5$ (Table III) are directly related to the quantum numbers of the ground-state and first excitations of chains of length $L = 4$ or 6 (respectively for the $N = 32$ and 36 samples). The effect of the transverse inter-chain coupling may be considered in a first approach as a minor quantitative effect. The lowest S=1 excitations consist of a set of 4 (N=16), 8 (N=32), respectively 6 (N=36) quasi degenerate states. Their parentage to the first excitation (labelled a in Table III) of the unique chain can be exactly traced back. Their wave vectors are vectors of the side of the square Brillouin zone (points k_5 and M of the Brillouin zone in Fig. 1 for $N = 36$) . Appropriate superpositions of these quasi degenerate states create S=1 excitations which are essentially localized on one given chain!
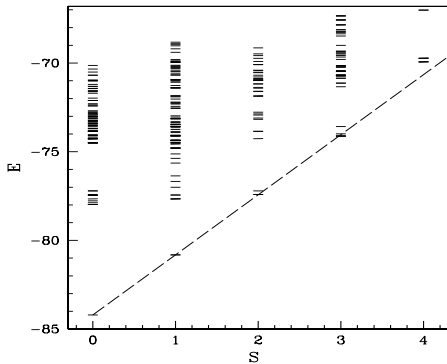

FIG. 8.   Same as Fig. 7 at $J_2/J_1 = 1.5$.

FIG. 7.   Spectrum of eigen-energies E in each total sector of spin S for $N = 36$ at $J_2/J_1 = 5$. This spectrum is quite close to the uncoupled chains one (see Table III). The lowest energies $E(S)$ in each S sector increase linearly with S up to $S = 3$ as shown by the dashed line.

The quasi degenerate states with total energy $\sim 77-78$ in Fig. 7 are associated to the creation of excitations with 2 "a-quanta" on different chains (levels 2a in Table III). This process gives birth to states with total spin $S = 0, 1, 2$. Endly we should notice that the linear increase with S of the lowest eigen-states in each spin sector is a last proof that one can add to the system up to 3 excitations of spin 1 (Fig. 7) which are essentially identical and have extremely weak interactions.

Decreasing the ratio J_2/J_1, the spectra testify of stronger interactions between multi-spinons excitations. In particular, a new feature does appear: a splitting of the singlet 2a excitations with a downward shift in energy of some of them which reach the level of the 1a-excitations at $J_2/J_1 = 1.5$ (Table III, Fig. 8 and Fig. 9). One can see in Fig. 9b this set of singlet states with excitation energy $\Delta E \sim 0.6J_2$ well separated from the other singlets. This is a new feature if we compare it to Fig. 9c for $J_2/J_1 = 5$, where the spectrum is merely that of uncoupled chains. But it is by no means related to the physics of the neighboring VBC phase as can be seen
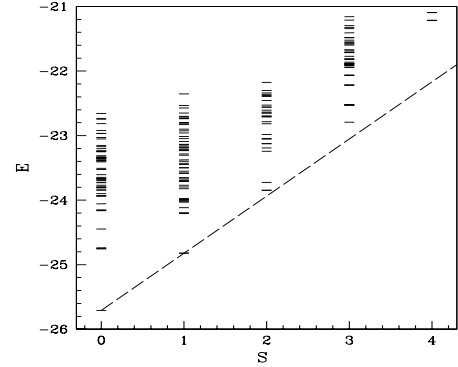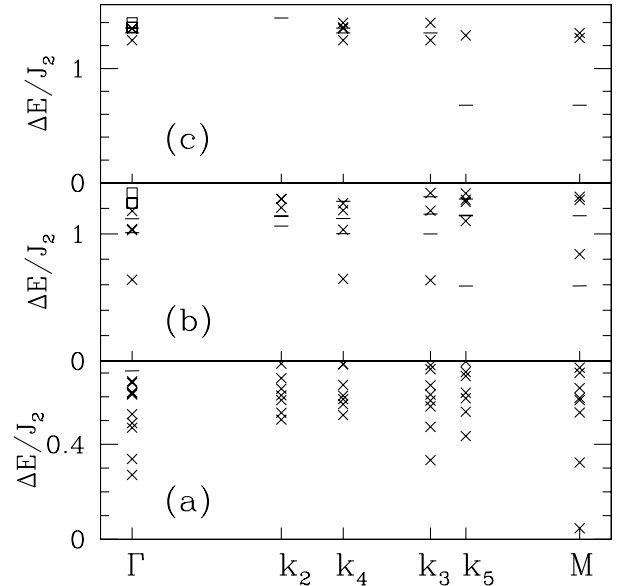

FIG. 9.   Lowest excitation energies above the ground-state $\Delta E/J_2$ vs wave vector k for $J_2 = 1$ (a) $J_2 = 1.5$ (b) $J_2 = 5$ (c) with spin $S = 0$ (crosses) , $S = 1$ (tirets) , $S = 2$ (open squares).

by comparing this spectrum with the VBC spectrum on the same sample Fig. 9a. As explained above the 1a-excitations can be described as purely "unidimensional", but these 2a-levels are excitations which cannot be localized on a single chain. The large energy gained with inter-chain coupling suggest some interrelation between chains. Yet the spin-spin and dimer-dimer correlations in these excitations are still strongly anisotropic as could be seen in Tables IV, V and Fig. 10. Note that the 2a-excitations occur at wave vectors which can be obtained by combining wave vectors of the 1a-excitations on the sides of the Brillouin zone. In the thermodynamic limit the 2a excitations are expected to cover densely the Brillouin zone. We conjecture that the appearance of these

—		1d						$J_2=5$				—			$J_2=1.5$		—
n	ΔE	S	k	σ		n	$\Delta E/J_2$	S	**k**	R	σ		n	$\Delta E/J_2$	S	**k**	R	σ
	0.	0	π	1			0.	0	Γ	-1	-1			0.	0	Γ	-1	-1
a	0.684741648	1	0	1		a	0.677944871	1	k_5		1		a	0.590054594	1	k_5		1
						a	0.677948816	1	M	i			a	0.591242101	1	M	i	
						2a	1.246710497	0	k_3		1		2a	0.635033794	0	k_3		1
						2a	1.246757039	0	k_4		1		2a	0.640143484	0	Γ	1	1
						2a	1.246757966	0	Γ	1	1		2a	0.645292084	0	k_4		1
b	1.302775637	0	0	-1		b	1.266511222	0	M	-1	-1		b	0.839974642	0	M	-1	-1
						b	1.288135982	0	k_5		-1		2a	1.000230994	1	k_3		-1
						b	1.309791780	0	M	1	-1		2a	1.001481120	1	k_4		1
						2a	1.309841802	1	k_3		-1		2a	1.008659631	1	Γ	-1	1
						2a	1.309846926	1	k_4		1		2a	1.029661098	0	Γ	-1	-1
						2a	1.309863513	1	Γ	-1	1		2a	1.032523222	0	k_4		-1
						2a	1.349565139	0	Γ	-1	-1		2a	1.037137527	0	Γ	1	-1
c	1.521999231	1	$2\pi/3$			2a	1.349566020	0	k_4		-1		c	1.060994796	1	k_2		-1
d	1.802775637	1	$\pi/3$			2a	1.349574718	0	Γ	1	-1		b	1.100373750	0	k_5		-1
						2a	1.352732556	1	Γ	i			2a	1.119357730	1	Γ	i	
						2a	1.352736474	1	k_4		-1		2a	1.120391023	1	k_4		-1
						2a	1.359019058	2	Γ	-1	-1		c	1.135860677	1	k_2		1
						2a	1.359020101	2	k_4		-1		c	1.142923268	1	k_2		-1
						2a	1.309863513	2	Γ	1	-1		3a	1.143097244	1	k_5		1
						2a	1.399283498	2	k_3		1		3a	1.143396461	1	M	i	
	2.802775637	2	π	1		2a	1.399292379	2	k_4		1		c	1.145902142	1	k_5		-1
	2.802775637	0	$\pi/3$			2a	1.399293748	2	Γ	1	1		2a	1.155611046	1	k_3		-1

TABLE III. Energy of excitations of the simple Heisenberg chain of length 6, of the CCM for $J_1 = 1$ and $J_2 = 5$ (respectively 1.5) on the $N = 36$ sample. For each eigen-state we display the total spin S, the **k** eigen-vector (as described in Fig. 1), the characters of the wave function respectively in a $\pi/2$ rotation (R) and in a mirror symmetry (σ). The index n indicates how the excitations of the 2d model can be build from excitations of the 1d Heisenberg chain.

excitations could be the precursor of a collective mode supposed to exist in a crossed sliding Luttinger liquid [13].

j	s(ij)		j	s(ij)
36	-0.4044253289		4	-0.0200188490
15	0.1666623287		2	-0.0403867716
22	-0.1505704767		9	0.0164521956
3	0.0505168767		16	-0.0129298755
10	-0.0536890650		17	0.0523125280
12	-0.0470765522			

TABLE IV. Spin-spin correlations in the 4th excited state of the spectrum at $J_2/J_1 = 1.5$. This state is one of the excited states of the 2-dimensional mode. As described in Table I it is a singlet state of the trivial RI ($\mathbf{k} = (0,0)$, $S = 0$, $R = 1$, $\sigma = 1$).

(k,l)	D		(k,l)	D
29 22	0.0421174442		35 30	-0.0043780206
22 15	-0.0099685219		11 6	-0.0043780208
31 6	0.0345888875		9 4	-0.0070999014
35 4	0.0055568217		17 10	0.0017481736
28 23	-0.0011288331		34 5	-0.0004575768
16 11	-0.0011288331		12 5	-0.0037470380
21 16	0.0139907353			

TABLE V. Dimer-dimer correlations in the 4th excited state of the $N = 36$ sample ($J_2/J_1 = 1.5$).

All these results (spectra, correlations, scaling of the spin gap) indicate a 1d behavior which extend down to $J_2/J_1 = 1.5$, i.e. well beyond the weak coupling limit investigated by (SSL). The 2-dimensional S=0 excitation mode singled out for $J_2/J_1 = 1.5$ on the N=36 sample may be an illustration of the collective mode of the " crossed sliding Luttinger liquid": it is highly anisotropic as could be expected. Its detailed properties should nevertheless be taken with some care due to the numerous constraints associated with periodic boundary conditions on these small samples.

The precise location of the lower limit of quasi 1d behavior is clearly out of reach of exact ED calculations. Nevertheless major modifications of the spectra when J_2/J_1 varies are a good qualitative indication of this transition.

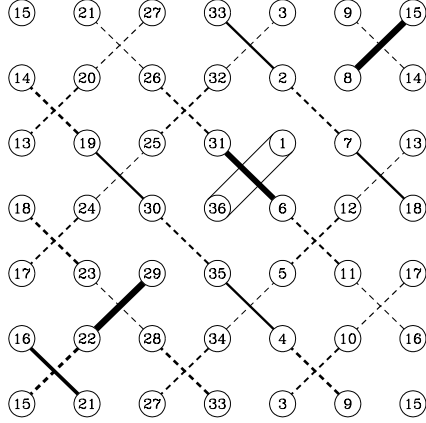At the isotropic point $J_2/J_1 = 1$ the ground-state is a

FIG. 10. Same as Fig. 5 in the 4th excited state of the N=36 sample ($J_2/J_1 = 1.5$).

VBC with LRO in 4-spin S=0 plaquettes [4]: this phase does not break $SU(2)$ symmetry (it has a spin gap), but breaks the space symmetry of the lattice. This last feature manifests itself by the existence of a very low lying $S = 0$ excited state which collapses to the ground-state in the thermodynamic limit. The absolute ground-state belong to the trivial irreducible representation of the space group (wave vector $k = (0,0)$, even in all operations of C_{4v}) and the first excited S=0 state, which embodies the VBC symmetry breaking is a state with wave-vector (π, π), odd under a $\pi/2$ rotation around O (These two states form the doublet called $\mathcal{E}_{VBC}$ in the following). When J_2/J_1 increases beyond 1, the first manifestation of the instability of the VBC phase appears in the modification of the symmetries of these low lying singlets, which is concomitant with the appearance of quasi 1-dimensional excitations in the S=1 sector: these two manifestations appear as soon as $J_2/J_1 = 1.05$ (resp 1.10) for $N = 32$ (resp 36). The transition shift to larger J_2/J_1 values with increasing sizes. Its location in the thermodynamic limit is difficult with present sizes. At $J_2/J_1 = 1.5$, as seen above, all characteristics (spectra and correlations functions) point to a sliding Luttinger liquid. At $J_2/J_1 = 1.25$, the scaling of the spin-gap (and the spectra) also suggest this behavior. The transition might occurs just below this point.

B. Coexistence of Néel LRO and VBC order

We now turn to the investigation of the extension of the Néel and the VBC phases and the question of their possible coexistence.

As discussed in [15,16] the simplest way to monitor the extension of Néel LRO is to search for the so-called quasi degenerated joint states (QDJS) which allow to break $SU(2)$ and lattice space symmetry in the thermodynamic

limit. This is a set of low lying states appearing in each total spin sector S up to $S \approx \sqrt{N}$, belonging to specific IRs of the space group, which collapse into a degenerate ground-state as $1/N$ for $N \to \infty$ and evolve as $S(S+1)$ with S. For collinear Néel LRO there is one QDJS for every S. Presently these states belong to the trivial IR of the space group for S even and to the $k = (0,0)$ IR, even under a mirror symmetry and odd under a $\pi/2$ rotation representation, when S is odd. In a plot of the spectrum vs $S(S+1)$ the QDJS form a line well separated from the macroscopic excitations (magnons) which only collapse as $1/\sqrt{N}$ as shown in Fig. 11 for $J_2 = 0$. The $\sim 1/N$ collapse of the QDJS implies that the spin-gap Δ also closes as $\sim 1/N$.

On the other hand the beginning of the plaquette phase may be estimated by the appearance of the quasi degenerate S=0 doublet ($\mathcal{E}_{VBC}$) sketched in the previous subsection.
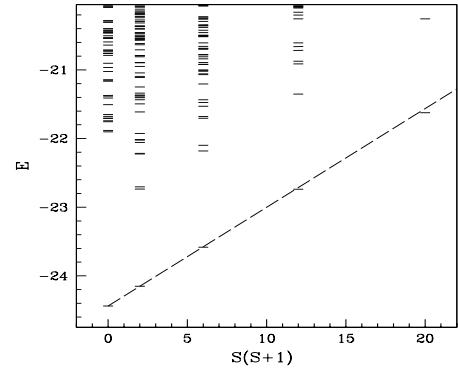

FIG. 11. Spectrum at $J_2 = 0$ (Heisenberg model on the square lattice) vs $S(S+1)$ for $N = 36$. The QDJS characteristic of collinear Néel LRO at the bottom of each S are well aligned (dashed line) and clearly separated from the other lowest excitations (see text).

The destruction of the QDJS and the appearance of $\mathcal{E}_{VBC}$ are not necessarily simultaneous. Both the Néel and the VBC phase may in principle co-exist in a gapless phase. In a recent paper Sachdev and Park [6], following earlier investigations in Ref [17], have suggested that the destabilization of collinear Néel LRO by 2th order transition into a VBC phase must generically occur within such a coexistence region.

Linear spin-wave calculations [2,3] predict that Néel LRO survive quantum fluctuations till $J_2/J_1 \approx 0.75$. Up to this value the characteristic features of Néel LRO are rather well observed in the spectra and in the evolution of Δ and E/N with N. Well below $J_2/J_1 = 0.75$, however, one may notice a slight curvature of the line of QDJS and there is small irregularity in the evolution of Δ and E/N with N: Δ is slightly larger and E/N slightly lower for $N = 36$ than for $N = 32$ as might be seen in Fig. 3 and Fig. 2. Nevertheless Δ seems to extrapolate rather well to zero at $N \to \infty$ at $J_2/J_1 = 0.65$. And for $J_2/J_1 =$
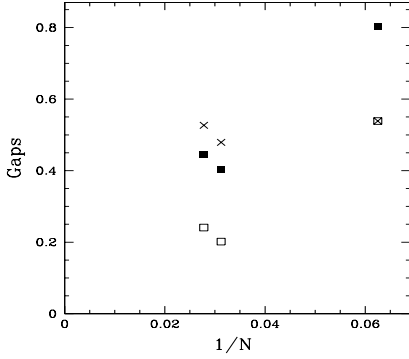
FIG. 12. Spin gaps Δ (full squares), separation of the two singlet states of $\mathcal{E}_{VBC}$ (open squares), gap between the ground-state and the third singlet (crosses) at $J_2/J_1 = 0.85$.

0.75 the $1/N$ extrapolation of the $N = 16, 32, 36$ values of Δ point to a spin-gap at most very small, ~ 0.06, a value of the order of the corrections to the asymptotic regime which are expected to be large and negative as we approach the boundary of the Néel phase [18,19]. So the Néel phase might persist up to this point. On the other hand, up to $J_2/J_1 = 0.75$, the separation of the two $\mathcal{E}_{VBC}$ states appears likely to remain finite as $N \to \infty$. Thus the VBC phase is not reached.

By contrast results at $J_2/J_1 = 0.85$ point to a finite spin gap and a degeneracy of the two states of $\mathcal{E}_{VBC}$ which remain separated from the other singlet states for $N \to \infty$ (Fig. 12).

These results lead to conclude to a transition between the two phases close to $J_2/J_1 \approx 0.75$ in agreement with the spin-waves result and that a coexistence region of the two phases either occurs at most in a very small range or is absent.

III. SUMMARY

Exact diagonalization have allowed to characterize three phases of the CCM: the (π, π) Néel phase at small diagonal couplings, 4-spin S=0 plaquette VBC at the isotropic point, and sliding Luttinger liquid for $J_2/J_1 \geq 1.25$. The transition between the Néel phase and the VBC phase occurs at $J_2/J_1 \approx 0.75$. No evidence of a coexistence region predicted by Sachdev and Park [6] is found. The CCM exhibits 1d behavior for a large range of parameters (J_2/J_1 greater than ≈ 1.25) where the transverse coupling between the chains is of the order of the intra-chain coupling. This 1d behavior is likely to be truly realizing the $SU(2)$ "Luttinger sliding phase" with deconfined spinons predicted by Starykh, Singh and Levine [1].

[1] O. A. Starykh, R. R. P. Singh, and G. C. Levine, Phys. Rev. Lett. **88**, 167203 (2002), cond-mat/0106260.
[2] R. Singh, O. A. Starykh, and P. J. Freitas, J. Appl. Phys. **83**, 7387 (1998).
[3] B. Canals, cond-mat/0102233 (unpublished).
[4] J.-B. Fouet, M. Mambrini, P. Sindzingre, and C. Lhuillier, cond-mat/0108070 (unpublished).
[5] W. Brenig and A. Honecker, cond-mat/0111405 (unpublished).
[6] S. Sachdev and K. Park, cond-mat/0108214 (unpublished).
[7] R. Coldea, D. A. Tennant, A. M. Tsvelik, and Z. Tylczynski, Phys. Rev. Lett. **86**, 1335 (2001).
[8] E. A. Axtell III, J. Solid State Chem. **134**, 423 (1997).
[9] S. R. White and I. Affleck, Phys. Rev. B **54**, 9862 (1996).
[10] A. A. Nersesyan, A. O. Gogolin, and F. H. L. Essler, Phys. Rev. Lett. **81**, 910 (1998).
[11] P. Azaria *et al.*, Phys. Rev. Lett. **81**, 1694 (1998).
[12] M. Bocquet *et al.*, Phys. Rev. B **64**, 094425 (2001).
[13] R. Mukhopadhyay, C. L. Kane, and T. C. Lubensky, Phys. Rev. B **64**, 045120 (2001) and C. L. Kane: March meeting talk 2002.
[14] A. Vishwanath and D. Carpentier, Phys. Rev. Lett. **86**, 676 (2001).
[15] P. Lecheminant *et al.*, Phys. Rev. B **56**, 2521 (1997).
[16] W. LiMing, G. Misguich, P. Sindzingre, and C. Lhuillier, Phys. Rev. B **62**, 6372 (2000).
[17] O. P. Sushkov, J. Oitmaa, and Z. Weihong, Phys. Rev. B **63**, 104420 (2001).
[18] P. Hasenfratz and F. Niedermayer, Z. Phys. B. Condensed Matter **92**, 91 (1993).
[19] J.-B. Fouet, P. Sindzingre, and C. Lhuillier, Eur. Phys. J. B **20**, 241 (2001).